

Development and Application of Coconut Vegetation Indices (CVIs) for Rapid and Accurate Coconut Mapping Using Sentinel-2 Images: A Case Study of Quezon Province, Philippines

John Erick J. Malangis¹, Ariel C. Blanco^{1,2}, Ayin M. Tamondong^{1,2}

¹ Department of Geodetic Engineering, University of the Philippines, Quezon City 1101, Philippines -
malangisjohnerick@gmail.com, {acblanco, amtamondong}@up.edu.ph

² Training Center for Applied Geodesy and Photogrammetry, University of the Philippines, Quezon City 1101, Philippines

Keywords: Coconut, Vegetation Index, Mapping, Remote Sensing, Sentinel-2

Abstract

The existing methods for coconut mapping in the Philippines and globally are complex, necessitating the development of a simpler yet rapid and accurate classification technique. This study introduces the first spectral index for coconut mapping. Two Coconut Vegetation Indices were developed: one for dense Coconut Vegetation (CV) and another for sparse CV. CVI_{dense} utilizes three Sentinel-2 bands in its equation (NIR1-SWIR1)/(SWIR1-SWIR2) to map coconut areas with densities $>2.25 \times 10^6$ sq.m. per 1km pixel. Meanwhile, CVI_{sparse} incorporates four spectral bands in the equation (NIR1-Red)/(SWIR1-SWIR2) for areas with densities $\leq 2.25 \times 10^6$ sq.m. per 1km pixel. The formulation of these indices is primarily based on previous studies involving band combinations and the analysis of spectral separability of the acquired coconut reflectance data. The extent of coconut vegetation was mapped using CVI_{dense} with a minimum threshold of 1.094, while CVI_{sparse} was applied using a threshold range of 0.4774 to 1.094. The Balanced Accuracy (BA) metric was used to assess the accuracy, accounting for the imbalanced reference data between coconut and non-coconut classes. CVI_{dense} proved highly effective with User's Accuracy (UA) of 80%, Producer's Accuracy (PA) of 88.89%, and BA of 88.90%, surpassing CVI_{sparse} , which had accuracies of 32.00% (UA), 53.33% (PA), and 74.10% (BA).

1. Introduction

The coconut (*Cocos nucifera L.*), a type of tree characterized as a fruit-bearing tree with a single stem and green, pinnate leaves, is native to tropical areas (Niral, V., et al., 2019). Coconut exerts a significant influence in the agricultural panorama of the Philippines, covering a total land area of 3.6 million hectares - encompassing 69 out of 82 provinces in the country (Philippine Coconut Authority, 2018). With this amount of land, the industry produces 14.7 million metric tons of coconut annually and contributes average export earnings of 91.4 billion pesos from 2014 to 2018 (Philippine Coconut Authority, 2018), which made it the world's top exporter (DA Press Office, 2023). These statistics underscore the Philippines as the second top coconut-producer in the world (Hoe, 2018).

Providing the largest part in the coconut production of the Philippines is Quezon Province which has a 10% share in the total supply nationwide and harvesting from approximately 60% of the province's total agricultural land area (SEARCA, 2023). More than 2,151 stakeholders in Quezon, including smallholder farmers, copra dealers, and traders in the province, rely directly on the coconut industry (SEARCA, 2023). Unfortunately, these stakeholders, specifically the farmers are struggling because of the climate crisis being evident in the extreme drought, intensified typhoons, and unexpected weather patterns (Lacerna, 2023). Infestation, low investments, limited research and development, and poor infrastructure were also determined as the factors that affect the declining farm yield that started in 2010 (DA Press Office, 2023). Given all these factors that are detrimental in the industry, it is therefore significant to monitor the current extent of coconut as affected by the said disturbances and limitations. Accurate spatial information regarding coconut plantations is crucial for managing natural resources and land-use planning. It is well established how significant remotely sensed data is for mapping, inventorying, and monitoring of natural resources (Kannan et al., 2017). Current studies on coconut

mapping explore the use of intensive and complex remote sensing techniques. These include the application of machine learning algorithms such as Convolutional Neural Network (CNN), Random Forest (RF), Support Vector Machine (SVM), and K-Nearest Neighbor (K-NN) (Ahmed et al., 2023; Vermote et al., 2020; Burnett et al., 2019). A recent study created a global density map of coconut plantations using a deep learning model, specifically semantic segmentation (Descals et al., 2023). Medium to very high-resolution images such as Sentinel-2 (Ahmed et al., 2023; Descals et al., 2023; Ian Jancinal et al., n.d.), WorldView-2 (Burnett et al., 2019) and WorldView-3 (Vermote et al., 2020) imageries have been used as sources of spatial information to map the extent of coconut vegetation in regional and global level. Other than this, Zheng et al. (2023) utilized Google Earth and deep learning models to detect individual coconut trees in remote atolls of the Pacific Ocean.

In the Philippines, coconut mapping is not a novel idea, however, it is still lacking with the very few studies exploring the accuracy of different detection and classification methods. The last land cover map of the Philippines to show the extent of coconut vegetation, together with other agricultural land cover, was made in 2016 through the Phil-LiDAR 2 program funded by the Department of Science and Technology (DOST) and jointly managed by the University of the Philippines Diliman (UPD) and the DOST Philippine Council for Industry, Energy, and Emerging Technology Research and Development (DOST-PCIEERD) (Pagkalinawan et al., 2017). One of its core projects, the Agricultural Resources Assessment (PARMap) project, focused on producing quality agricultural maps using Light detection and ranging (LiDAR) technology and Landsat data (Pagkalinawan et al., 2017). Bernales et al. (2016) also applied the use of LiDAR and SVM in coconut tree detection in the Municipality of Mambusao in Capiz, Philippines. The same LiDAR technology was utilized to assess and map agricultural resources, including coconuts,

in Bacolod, Lanao Del Norte (Guiahwan et al., 2018), and the Davao Region (Novero et al., 2019).

None of the previous projects and studies explored the feasibility, development, and application of a spectral index that is specific to coconut vegetation, which could provide simple, direct, and accurate mapping of coconut areas. Spectral indices used in mapping vegetation are called vegetation indices. The indices such as the Normalized Difference Vegetation Index (NDVI; Rouse et al., 1973), Soil Adjusted Vegetation Index (SAVI; Huete, 2004), and Leaf Area Index (LAI) are useful in highlighting intrinsic plant properties that are strongly associated with leaf greenness and vigor (Baloloy et al., 2020). There are also indices made for specific vegetation such as Mangrove Vegetation Index (MVI) (Baloloy et al., 2020) and Rice Growth Vegetation Index (RGVI) (Nuarsa et al., 2011), which made the mapping of vegetation easier and without the need for data-intensive methodologies, complex classifiers, and skill-dependent classification techniques.

Lastly, given the complexities in the current coconut mapping techniques and the absence of vegetation index for coconut, this study proposed a simplified method using the first Coconut Vegetation Index (CVI) that uses the Red, NIR, SWIR-1, and SWIR-2 bands of Sentinel-2. Two CVIs specific to dense (closed-canopy) and to sparse (open-canopy) vegetation were developed in the study. The index was designed by analyzing the spectral signatures and characteristics of coconut (in dense and sparse vegetation) and non-coconut datasets for Quezon Province.

2. Methodology

For this study, the methodology was structured into two parts. The first part was dedicated to analyzing the varying spectral responses of Sentinel-2 bands between the coconut and non-coconut pixels. Two CVIs were developed in this study, thus various combinations of bands were tested separately for dense and sparse coconut vegetation. Subsequently, the CVIs were applied to Sentinel-2 images covering the study site. The second part of this study focused on mapping coconut extent using the CVIs, along with accuracy assessment using available submeter satellite images. Figure 2 highlights the general workflow of this study.

2.1 Study Site

Quezon Province, centered at 13.9347 N, 121.9473 E, is the target area for this study. It is the 9th largest province in the country, with a total area of 8,743.84 sq. km., and the 13th most populated, home to 1,950,459 citizens as of 2020. The province has consistently been a leader in Region IV-A (CALABARZON) in terms of agricultural exports. The Philippine Statistics Authority (PSA) recorded that 35.3% of the 2022 Agricultural, Forestry, and Fishing (AFF) exports came from Quezon.

Figure 1 illustrates the spatial distribution of coconut density across the province. The coconut industry is a major contributor to the province's economy, with copra making being cited as "one of the largest income-generating agricultural activities in the province." It has long been considered the coconut capital of the Philippines, and the largest coconut-producing province (Pabuayon et al., 2009). In 2020, the Local Government Unit (LGU) of Quezon reported that the province produced 1,493,066.64 metric tons of

coconuts. Quezon's land area is mostly agricultural, occupying 47.87% or 4,167.6421 sq. km. Out of these, 3,791.376 sq. km. are dedicated to coconut plantations, also making it the province with the largest coconut production area.

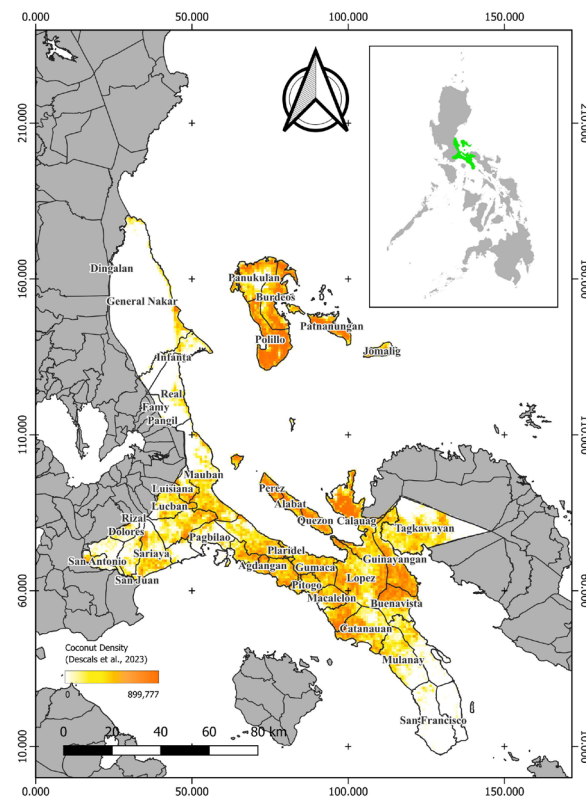


Figure 1. Map of Quezon Province with an overlay of coconut density distribution from Descals et al. (2023)

2.2 Datasets

Data	Source	Resolution	Time Period
Sentinel-2 – L2A Images	Copernicus Data Space Ecosystem	10m; 20m	2020
Training Data for Spectral Analysis and Threshold Development	Google Earth	-	-
Reference/Validation Data	Google Earth	-	-
Global Closed-Canopy Coconut Map	Descals et al. (2023)	20m	2020

Table 1. Summary of Data

To conduct this study, Sentinel-2 L2A images with minimal cloud cover were downloaded from the Copernicus Data Space Ecosystem. L2A was preferred over L1C for its open access and atmospheric correction. Coconut and non-coconut samples for spectral signature generation and validation were extracted from Google Earth, which offers open-access, high-resolution imagery. Additionally, the global closed-canopy coconut map by Descals et al. (2023) was used to guide sample selection across varying vegetation densities. A summary of all datasets used in this study is presented in Table 1.

2.3 Workflow

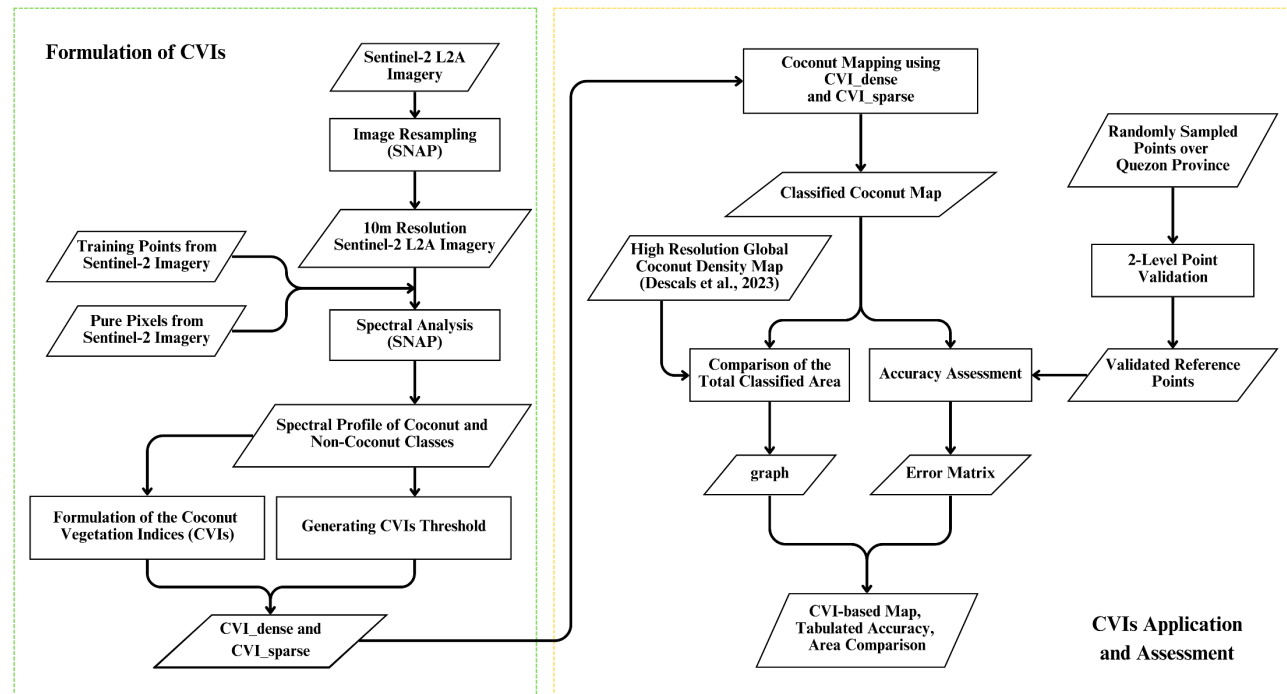


Figure 2. General workflow that highlights the main parts of the methodology: formulation of CVIs and its application

2.4 Formulation of CVIs

2.4.1 Spectral Analysis and Development of CVIs: The spectral bands that were mainly assessed in the formulation of the index were derived from the resampled Sentinel-2 images (10m resolution) acquired over Quezon Province. The training points were selected using Google Earth. One hundred training points (100) (Baloloy et al., 2020) were collected for coconut (dense and sparse) and non-coconut pixels (forest and non-terrestrial vegetation). The Sentinel Application Platform (SNAP) was utilized to generate the spectral profiles and extract the reflectance of the points from Sentinel-2 images.

Since the spectral signature of dense and sparse coconut vegetation has a huge difference that coincides with other non-coconut classes (See Figure 4), this study created two spectral indices not only specific for coconut vegetation but also to its density and structure of tree cover.

2.4.2 CVIs Threshold: Using Sentinel-2 images, Google Earth, and the global closed-canopy coconut map (Descals et al., 2023), 50 training samples (Baloloy et al., 2020) for each land-use and land-cover class were selected within the boundaries of Quezon Province. Each training pixel represents a pure sample of the given class, and its spectral profiles were also considered in developing the CVIs. Each pixel's purity was assessed using the following criteria:

1. Sub-meter satellite images are available to identify the vegetation.
2. The pixel should be within the center of the vegetation's extent to ensure that no other land cover will affect its purity.
3. In the case of the dense CV, the pixel should fall within the area with $> 2.25 \times 10^6$ sq. m. of coconut per pixel defined by Descals et al.'s (2023) coconut density map.

However, in the case of sparse CV where it is highly influenced by other vegetation or non-vegetation classes and the purity of its pixel does not adhere to the standard definition,

the following criteria was set in this study to achieve consistency:

1. A sub-meter satellite image is available to identify the sparse CV pixel.
2. It falls within the area with $\le 2.25 \times 10^6$ sq. m. of coconut per pixel defined by Descals et al.'s (2023) coconut density map.
3. Only one coconut tree is within the 10-m pixel range.

The mean, upper, and lower thresholds for sparse coconut, dense coconut, and non-coconut were determined by producing CVIs for the following classes: coconut (sparse and dense), terrestrial vegetation (forest and non-forest), bare soil, water, built-up, and clouds (Baloloy et al., 2020).

2.5 Application of CVIs to Sentinel-2 Images

For the index computation, the mosaic of resampled (into 10m resolution) Sentinel-2 L2A images was used as the input. The CVI formulas were applied to the image using the Raster Calculator in QGIS Firenze 3.28.15. Following that, the CVI outputs were filtered to select just the pixels within the dense and sparse coconut using the determined threshold values. The results of both CVIs were integrated into a single image to assess the combined accuracy.

2.6 Validation of Reference Points

Six hundred (600) reference points (Burnett et al., 2019) were randomly sampled over Quezon Province using the Random Points in QGIS Firenze 3.28.15. These points were then validated in two levels. The first one is the validation by the author and the second level is the validation by an independent interpreter (Descals et al., 2023). Table 2 shows the criteria for classifying the reference points as adapted from the study of (Descals et al., 2023).

Class	Description
0	Land Cover could not be determined because sub-meter resolution data were not available, or it is partially or fully covered by clouds. Non-Vegetation Area but with coconut tree/s within 10 m pixel Vegetation Area but with coconut tree/s within 10m pixel
1	Non-Vegetation Area (e.g. bare soil / built-up) indicates that vegetation coverage is < 50% and coconut trees are not within the 10 m pixel
2	Vegetation Area (e.g. forest or non-forest trees) indicates that vegetation coverage is > 50% and coconut trees are not within the 10 m pixel
3	Sparse coconut trees indicate a low density of coconut vegetation. There are one or two coconut trees within the 10m pixel. The point is within the light yellow area ($\leq 2.25 \times 10^6$ sq. m. of coconut per pixel) of the Coconut Density Map of Descals et al. (2023).
4	Dense coconut tree indicates a high density of coconut vegetation. There are more than two coconut trees within the 10m pixel. The point is within the orange area ($> 2.25 \times 10^6$ sq. m. of coconut per pixel) of the Coconut Density Map of Descals et al. (2023).

Table 2. Criteria for Point Validation as adapted from the study of Descals et al. (2023)

Reference images, as shown in Figure 3, were incorporated into the level 2 validation to help limit the potential errors in image interpretation. In cases where there was a mismatch between the interpretation of the author and the independent interpreter, both individuals deliberated to come up with the final class to assign.

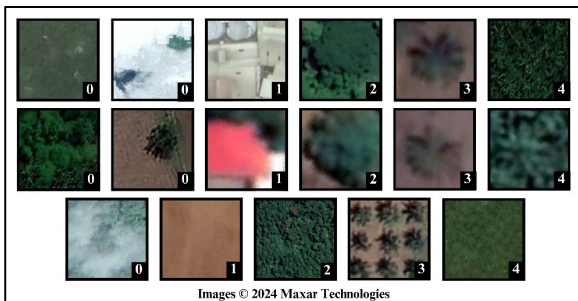


Figure 3. Reference photos that were used for validation by the independent interpreter. The number in the photos correspond to its class

2.7 Index Accuracy Assessment

A separate assessment for the two CVIs was conducted to determine their individual performance. Other than the Producer's Accuracy (PA), User's Accuracy (UA), and Overall Accuracy (OA), the Balanced Accuracy (BA) was also computed to consider the imbalance number of reference points between the coconut and non-coconut classes. The metric accounts for both false positive and false negative errors that have a direct impact on the targeted class (Mower, 2005). Equation 1 shows the necessary parameters in the computation of the BA.

$$\text{Balanced Accuracy (BA)} = \frac{TPR + TNR}{2}, \quad (1)$$

where:

$$\text{True Positive Rate (TPR)} = \frac{\text{True Positive (TP)}}{\text{TP} + \text{False Negative}} \quad (2)$$

and

$$\text{True Negative Rate (TNR)} = \frac{\text{True Negative (TN)}}{\text{TN} + \text{False Positive}} \quad (3)$$

In this study, a true positive refers to the number of reference coconut pixels that were also classified as coconut using the indices, while true negative is the number of misclassified coconut pixels. Furthermore, false negative is the number of reference non-coconut pixels that were classified as coconut, and a false positive refers to the number of non-coconut pixels that were also classified as its class using the indices.

To further address the classification accuracy of the indices, omission errors and commission errors were also computed through the following equations:

$$\text{Omission Error} = 100\% - \text{Producer's Accuracy} \quad (4)$$

$$\text{Commission Error} = 100\% - \text{User's Accuracy} \quad (5)$$

Accuracy assessment of the result upon application of the two CVIs in one image was also conducted to determine the overall performance of its integration.

3. Results and Discussion

3.1 Coconut Vegetation Indices

This study proposed to use the following spectral bands: red, NIR1, SWIR1, and SWIR2, as components of the coconut vegetation index. Ahmed et al. (2023) and Descals et al. (2023) demonstrated that these bands can accurately classify coconut vegetation from other land cover using different classification algorithms.

On the other hand, as observed in Figure 4, the spectral signatures of dense and sparse coconut vegetation (CV) have huge differences in the visible region as well as in SWIR1 and SWIR2 bands, which can be attributed to the background environment of these vegetations. Thus, this study developed two vegetation indices that are specific to dense CV and sparse CV.

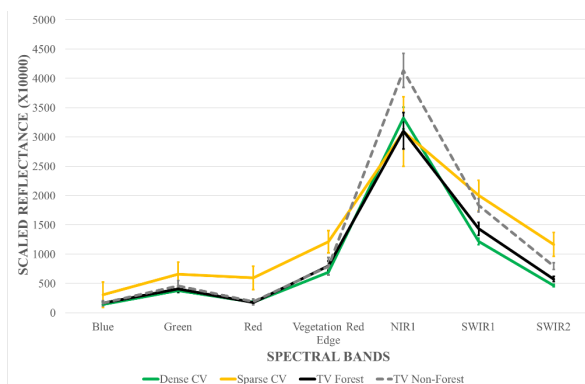


Figure 4. Spectral profile of coconut and non-coconut classes.

3.1.1 Coconut Vegetation Index for Dense Plantation: The CVI for dense coconut plantations utilized NIR1, SWIR1, and SWIR2, with central wavelengths of 0.842 μm, 1.610 μm, and 2.190 μm, respectively. Figure 4 shows that dense CV has the lowest reflectance in SWIR bands among all land covers. With this, the sum of the SWIR bands will always be smaller in dense CV compared to the other land covers. This combination, given that SWIR bands are sensitive to moisture, enhances the detection of coconut trees, which have naturally waxy cuticles covering their leaves to maintain the moisture content as a unique adaptation response to drought (Carr, 2011).

Since dense CV is defined as a closed canopy with high density of coconut trees, the environment below the canopy cover will not greatly affect the reflectance values, and only the features of the tree crown will be reflected. Equation 6 shows the CV index for dense coconut areas.

$$CVI_{dense} = \frac{NIR1 - SWIR1}{SWIR1 + SWIR2} \quad (6)$$

where:

NIR1 = Near Infrared 1 Reflectance (0.842 μm)

SWIR1 = Short-Wave Infrared 1 Reflectance (1.610 μm)

SWIR2 = Short-Wave Infrared 2 Reflectance (2.190 μm)

Meanwhile, the spread of NIR1 reflectance of dense CV might overlap with terrestrial vegetation (TV) in forest and sparse CV as shown in Figure 4. This can be attributed to the same amount of chlorophyll concentration and health condition of the vegetation types (see Figure 5). To resolve this, SWIR1 was combined with NIR to treat the latter like a constant for all classes since the former is more separable and has narrower spread based on its standard error.

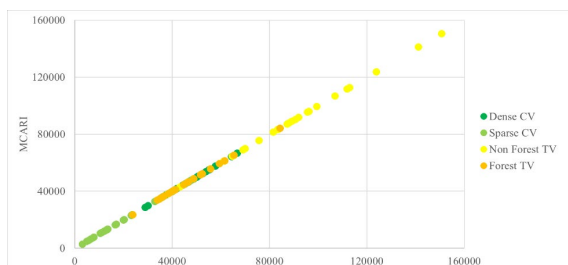


Figure 5. Modified Chlorophyll Absorption in Reflectance Index (MCARI) of coconut and terrestrial vegetation.

3.1.2 Coconut Vegetation Index for Sparse Plantation: In this study, sparse CV is defined as the open canopy and low-density coconut tree plantation. With this, its background environment significantly affects its reflectance values. The high values of SWIR bands could be attributed from the soil or the ground within the background.

$$CVI_{sparse} = \frac{NIR1 - Red}{SWIR1 + SWIR2} \quad (7)$$

where:

NIR1 = Near Infrared 1 Reflectance (0.842 μm)

Red = Red Reflectance (0.665 μm)

SWIR1 = Short-Wave Infrared 1 Reflectance (1.610 μm)

SWIR2 = Short-Wave Infrared 2 Reflectance (2.190 μm)

For the case of sparse CV, the sum of its SWIR bands will always be higher than the other land covers. Meanwhile, the average difference between the NIR1 and Red (with a central

wavelength of 0.665 μm) will always be smaller compared to the other classes. The inclusion of NIR1 and Red considers the effects of the background environment to the register of the tree cover in satellite images since sparse CVs are usually surrounded by bare soil or grassy areas.

The proposed indices in this study are the first coconut indices for coconut mapping. Existing studies show the use of LiDAR or satellite images with machine or deep learning models (Candare et al., 2016; Saavedra et al., 2016; Guihawan et al., 2018; Burnett et al., 2019; Novero et al., 2019; Bernales et al., 2022; Descals et al., 2023; Ahmed et al., 2023; Xi et al., 2023) which are way complex and data-intensive compared to using a spectral index.

3.2 CVIs Threshold

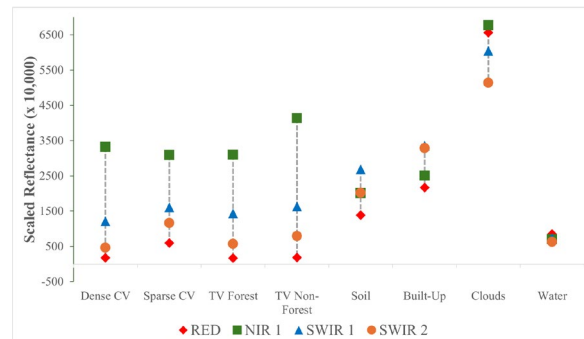


Figure 6. Separation of selected bands per class

3.2.1 Threshold for CVI_{dense} : The CVI_{dense} values of pixels identified as coconut (dense and sparse), terrestrial vegetation (forest and non-forest), bare soil, built up, water and clouds were plotted in Figure 6. The mean of CVI values for dense plantation is 1.2549, with maximum value of 1.6052 and minimum value of 1.0940. The whole extent of this threshold is separated from the threshold of terrestrial forest and non-forest vegetation, with maximum threshold up to 0.9885. This is the result of the distinct spectral response of dense coconut vegetation in the NIR1, SWIR1, and SWIR2 wavelengths. Maximizing the numerator (NIR1-SWIR1) and minimizing the denominator (SWIR1 + SWIR2) yields higher CVI_{dense} values. Figure 7 provides a comparative summary of index threshold values applied across different classes.

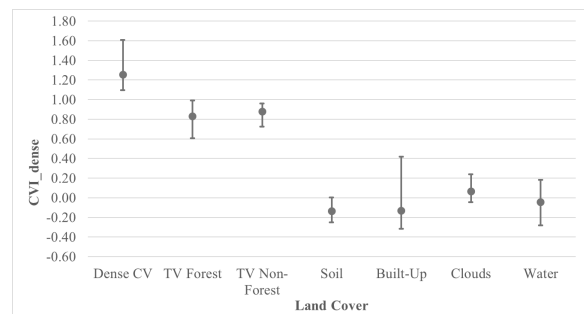


Figure 7. Mean, minimum and maximum CVI_{dense} values of dense coconut and non-coconut pixels: terrestrial vegetation – forest (TV Forest), terrestrial vegetation-non forest (TV Non-Forest), bare soil, built-up, water, and clouds

Meanwhile, the CVI_{dense} values of bare soil and built-up ranges from -0.2506 to -0.0006 and -0.3177 to 0.4159, respectively. Both classes exhibit high reflectance values in the SWIR region. The SWIR reflectance of soil is significantly influenced by the mineral composition, organic matter, and

surface water content (Sykas, 2020). The high reflectance of built-up areas in the SWIR region is primarily due to urban surfaces and artificial materials (Baloloy et al., 2020). With higher SWIR1 values than NIR1, the numerators of the CVI_{dense} for soil and built-up classes are smaller. However, the CVI_{dense} 's denominator is smaller because the SWIR2 values are either smaller (in bare soil) than or almost the same (in built-up) of the SWIR1.

3.2.2 Threshold of CVI_{sparse} : Unlike the dense coconut vegetation, the threshold of sparse coconut vegetation is between terrestrial vegetation and the other land cover, as clearly illustrated in Figure 8. The mean of CVI_{sparse} values is 0.7956, with maximum of 1.0940 and minimum of 0.4774. This is smaller than the TV forest which has a minimum of 1.2302. This is because of the high SWIR2 reflectance that makes the denominator of the index higher than those of the other classes. The whole extent of this threshold is separated from all the other land covers. This is the result of combining NIR1, Red, and SWIR bands that reveal distinct spectral signatures for sparse CV. To generate more separable CVI_{sparse} values, the band combinations should produce values that are closer to the mean.

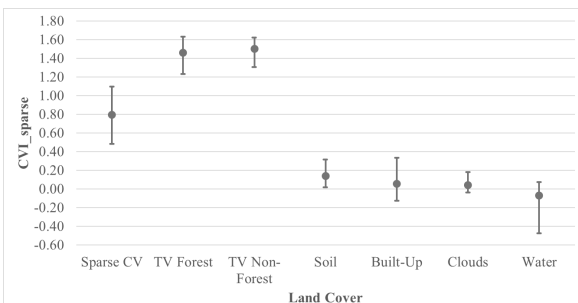


Figure 8. Mean, minimum and maximum CVI_{sparse} values of dense coconut and non-coconut pixels: terrestrial vegetation – forest (TV Forest), terrestrial vegetation-non forest (TV Non-Forest), bare soil, built-up, water, and clouds

Meanwhile, bare soil and built-up shows lower values than the CVI_{sparse} with a maximum of 0.3112 and 0.3324, respectively. These classes register smaller index values than the sparse CV. This could be attributed to the high values of the component bands, which are all higher than the coconut and terrestrial vegetation.

3.3 Generated CVI-Based Map and Images

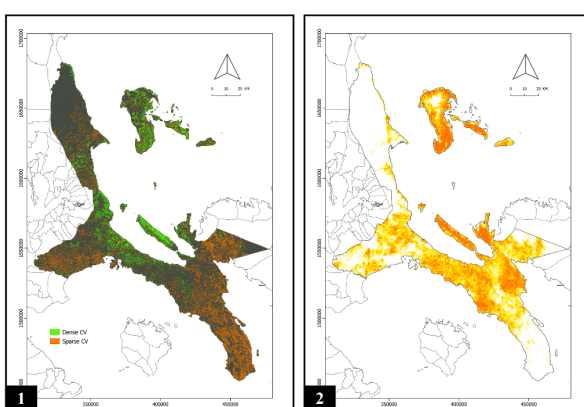


Figure 9. Maps showing the extent of (1) whole coconut vegetation in Quezon Province using CVIs and the (2) 20-m

resolution coconut density map created by Descals et al. (2023) using data from the same year as this study, 2020

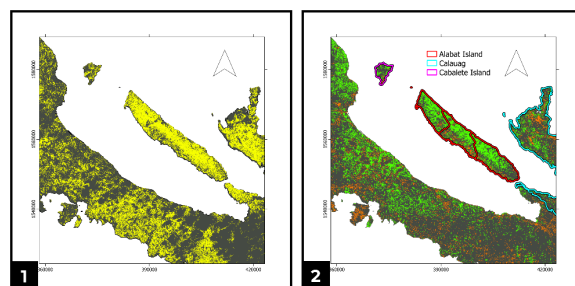


Figure 10. Maps showing the extent of coconut vegetation which were produced using (1) Landsat-8 and SVM Classifier (Tañada et al., 2023), and (2) CVIs. Despite method (1) utilizing a satellite image from 2013-2015 and the other using images from 2020, significant similarities in coconut vegetation extent are observed across Alabat Island, Cabalete Island, and areas in Calauag

As shown in Figures 9 and 10, dense coconut areas in Calauag and on the islands of Alabat, Cabalete, Polillo, and Patnanungan were also classified using CVI_{dense} , consistent with the coconut density map by Descals et al. (2023) and the coconut vegetation map by Tañada et al. (2023). Some dense areas, however, remained unclassified due to persistent cloud cover in the imagery (see Figure 11). Since this study used Sentinel-2 images with remaining cloud cover, clouds likely obscured portions of the canopy, resulting in missed or misclassified pixels. This limitation emphasizes the need for cloud-free composites or multi-temporal imagery in future analyses to improve classification completeness. In the upper part of the classified map, the non-coconut pixels correspond to those identified by Descals et al. (2023). However, the area within the Bondoc Peninsula shows classified sparse vegetation which is barely present in the reference map. The 10m spatial resolution of Sentinel-2 allows finer delineation of sparse CV. Figures 12 and 13 illustrate finer spatial details of the classified dense and sparse coconut vegetation.

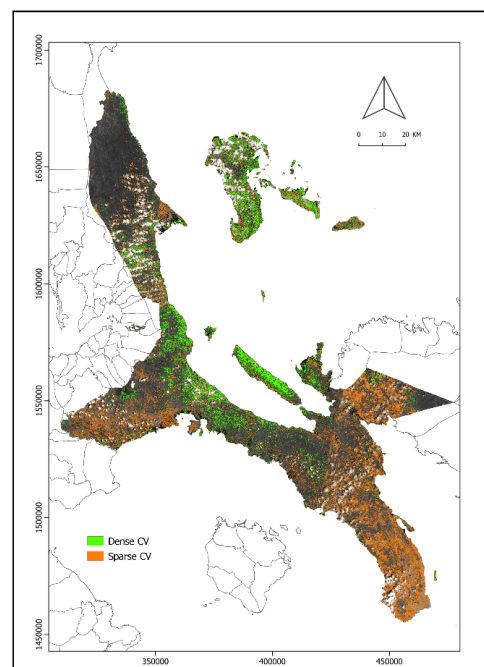


Figure 11. CVI-based maps with cloud cover

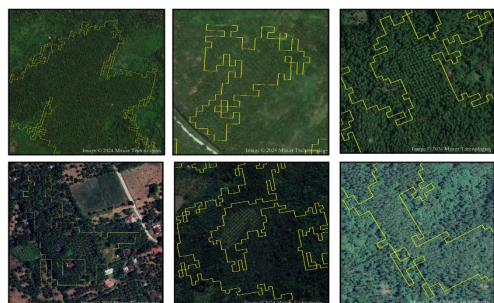


Figure 12. CVI_{dense} -classified coconut plantations that are within the sites of highest coconut density according to Descals et al. (2023)



Figure 13. Coconut plantations that were classified using CVI_{sparse}

3.4 Index Accuracy

Spectral Index	UA	PA	OA	BA
CVI_{dense}	80.00%	88.89%	94.60%	88.90%
CVI_{sparse}	32.00%	53.33%	74.10%	60.83%
Integrated CVI	51.20%	71.11%	73.07%	69.03%

Table 3. Accuracy of the mapped coconut areas using CVIs

After examining the sampled reference points, a total of 287 points were validated as part of coconut and non-coconut classes. Forty-five (45) points belong to the dense CV, nine (9) for sparse CV, 192 for vegetation area (terrestrial and non-terrestrial), and the non-vegetation area (bare soil and built-up) has 41 points. Since the number of validated points for sparse CV is too small for the study site, an additional 36 points were validated to match the points for dense CV.

CVI_{dense} exhibited the highest accuracy among the classifiers, with User's, Producer's, Overall, and Balanced Accuracies all above 80.00%. It recorded the lowest omission (11.11%) and commission (2%) errors for coconuts, and less than 5% for non-coconut classification. In contrast, CVI_{sparse} showed the lowest accuracy, with 68% commission and 53.33% omission errors for coconuts, reflecting the known challenge of delineating sparse CV due to the impact of other land covers on its reflectance (Descals et al., 2023).

The notably higher Overall Accuracies compared to UA and PA are due to the imbalance in reference data, with dense coconut samples outnumbering sparse class. This imbalance can bias results toward the majority class, reducing detection reliability for underrepresented categories. Balanced Accuracy was therefore calculated, and future work should address this issue through more balanced sampling or resampling techniques.

3.5 Area Comparison

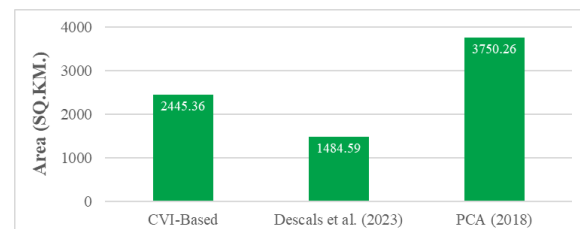


Figure 14. Area of coconut vegetation in Quezon Province based on CVI, the density map of Descals et al. (2023), and the data from PCA (2018)

Using CVIs, the extent of coconut vegetation in Quezon Province reached up to 2445.36 sq. km., exceeding Descals et al.'s (2023) categorized area of 1484.59 sq. km. Both computed areas are smaller than PCA's 2018 record of 3750.26 sq. km. The low classified area can be attributed to the cloud cover in satellite images used in this study. Misclassified pixels among coconut and non-coconut were factors in these values as also affected by the low accuracy of CVI_{sparse} .

4. Conclusion and Recommendations

This study developed two spectral indices to delineate dense and sparse coconut vegetation (CV) based on their distinct spectral signatures. The dense CV index, using NIR1 and SWIR bands, achieved the highest accuracy of more than 80%. The sparse CV index, using NIR1, Red, and SWIR bands, showed lower accuracy, highlighting the difficulty in mapping sparse CV. The CVI-based map estimated a greater coconut extent than earlier studies but remained smaller than PCA records, suggesting a more refined yet improvable delineation.

These findings demonstrate the potential of the developed vegetation indices to support the PCA in nationwide coconut monitoring using spatial data and mapping. Such capability is valuable for rapid assessment of typhoon impacts and can also inform planting and replanting strategies aimed at enhancing long-term productivity and economic resilience.

Future work should apply the indices to Sentinel-2 L2A (20 m resolution), explore other sensors (e.g., Landsat), expand spatial coverage, and increase the training and reference data. Differentiating coconut from oil palm using spectral analysis, ground-truth validation, and integrating texture features, Synthetic Aperture Radar (SAR) data, and high-resolution drone imagery are also recommended to enhance mapping accuracy and reliability.

References

Ahmed, Z., Nageswara Rao, P. P., & Srikanth, P., 2023: Area Estimation of Mango and Coconut Crops using Machine Learning in Hesaraghatta Hobli of Bengaluru Urban District, Karnataka. *Journal of Geomatics*, 17(1), 85–92. doi.org/10.58825/jog.2023.17.1.75.

Baloloy, A. B., Blanco, A. C., Raymund Rhommel, R. R. C., & Nadaoka, K., 2020: Development and application of a new mangrove vegetation index (MVI) for rapid and accurate grove mapping. *ISPRS Journal of Photogrammetry and Remote Sensing*, 166, 95–117. doi.org/10.1016/j.isprsjprs.2020.06.001.

Bernales, A. M. J., Samonte, C. O., Antolihao, J. A. F., Silapan, J. R., Edullantes, B., Pada, A. V. S., & Dela Serna, A.

M. L., 2016: Integration of Template Matching and SVM Technique for Coconut Tree Detection. *37th Asian Conference on Remote Sensing. Asian Association on Remote Sensing*. <https://bit.ly/49gAlxa>.

Burnett, M. W., White, T. D., McCauley, D. J., De Leo, G. A., & Micheli, F., 2019: Quantifying coconut palm extent on Pacific islands using spectral and textural analysis of very high resolution imagery. *International Journal of Remote Sensing*, 40(19), 7329–7355. doi.org/10.1080/01431161.2019.1594440.

Carr, M. K. V., 2011. The Water Relations and Irrigation Requirements of Coconut (*cocos nucifera*): A Review. *Experimental Agriculture*, 47(1), 27–51. doi.org/10.1017/s0014479710000931.

DA Press Office., 2023: DA wants to boost coconut industry productivity to benefit millions of farmers. Official Portal of the Department of Agriculture; Department of Agriculture. <https://www.da.gov.ph/da-wants-to-boost-coconut-industry-productivity-to-benefit-millions-of-farmers> (20 March 2024).

Descals, A., Wich, S., Szantoi, Z., Struebig, M. J., Dennis, R., Hatton, Z., Ariffin, T., Unus, N., Gaveau, D. L. A., & Meijaard, E., 2023: High-resolution global map of closed-canopy coconut palm. *Earth System Science Data*, 15(9), 3991–4010. doi.org/10.5194/essd-15-3991-2023.

Guiahwan, J., Tabugo, S. R., Amparado, R., & Burlat, C., 2018: Mapping of Agricultural and Coastal Resources in the Municipality of Bacolod, Lanao del Norte using LiDAR datasets and GIS. *International Conference on Environment and Forest Conservation 2018*. <https://bit.ly/4ncSQ97>.

Hoe, T. K., 2018: The Current Scenario and Development of the Coconut Industry. *The Planter*, 94 (1108), 413–426. <http://bit.ly/3WRS4nf>.

Jancinal, J. I. L., Corvera, J. B., & Cauba, A. G., Jr., 2023: Mapping Coconut Trees And Its Production Of Virgin Coconut Oil Within Butuan City, Philippines Using Sentinel-2 Data. *44th Asian Conference On Remote Sensing, Acrs 2023*. <http://bit.ly/3JmXfbH>.

Kannan, B., Ragunath, K. P., Kumaraperumal, R., Jagadeeswaran, R., & Krishnan, R. (2017). Mapping of coconut growing areas in Tamil Nadu, India using remote sensing and GIS. *Journal of Applied and Natural Science*, 9(2), 771–773. doi.org/10.31018/jans.v9i2.1272.

Lacerna, S. A., 2023: Quezon farmers struggle for climate resilient coconut industry. *The Philippine Star*. <https://philstar.com/headlines/climate-and-environment/2023/11/23/2313689/quezon-farmers-struggle-climate-resilient-coconut-industry> (12 December 2023).

Niral, V., Samsudeen, K., Sudha, R., Ranjini, T.N., 2019. Genetic resource management and improved varieties of coconut. *Ind. Coconut J. ICAR-CPCRI Kasargod* <https://krishi.icar.gov.in/jspui/bitstream/123456789/24188/1/Genetic%20Resource%20Management%20and%20Improved%20Varieties%20of%20Coconut.pdf> (12 December 2023).

Novero, A. U., Pasaporte, M. S., Aurelio, R. M., Madanguit, C. J. G., Tinoy, M. R. M., Luayon, M. S., Oñez, J. P. L., Daquiao, E. G. B., Diez, J. M. A., Ordaneza, J. E., Riños, L. J., Capin, N. C., Pototan, B. L., Tan, H. G., Polinar, M. D. O., Nebres, D. I., & Nañola, C. L., 2019: The use of light detection and ranging (LiDAR) technology and GIS in the assessment and mapping of bioresources in Davao Region, Mindanao Island, Philippines. *Remote Sensing Applications: Society and Environment*, 13, 1–11. doi.org/10.1016/j.rsase.2018.10.011.

Nuarsa, I. W., Nishio, F., & Hongo, C., 2011: Spectral characteristics and mapping of rice plants using multi-temporal Landsat data. *Journal of Agricultural Science*, 3(1). doi.org/10.5539/jas.v3n1p54.

Pabuayon, I. M., Medina, S. M., Medina, C. M., & Manohar, E. C., 2009: The Philippines' Regulatory Policy on Coconut Cutting: An Assessment Incorporating Environmental Consideration. *Journal of the International Society for Southeast Asian Agricultural Sciences*, 15 (2), 93–106. <https://api.semanticscholar.org/CorpusID:55438149> (2 February 2024).

Pagkalinawan, H. M., Gatdula, N. B., Jose, R. P., Rollan, T. M., Tañada, E. M., Magtala, S. Y., Dela Torre, D. G., Dela Cruz, P. A., Aves, J. L., Tan, G. D., Apura, R. A., Dimalanta, C. P., & Blanco, A. C., 2017: Quality assessment and control of outputs of a nationwide agricultural land cover mapping program using LiDAR: Phil-LiDAR 2 PARMap experience. *International Archives of the Photogrammetry, Remote Sensing and Spatial Information Sciences - ISPRS Archives*, 42(3W2), 163–170. doi.org/10.5194/isprs-archives-XLII-3-W2-163-2017.

Philippine Coconut Authority, 2018: Coconut Statistics. <https://pca.gov.ph/index.php/resources/coconut-statistics> (12 December 2023).

SEARCA, 2023: Development of the coconut industry growth areas in the province of Quezon. [Searca.org; SEARCA](https://www.searca.org/projects/research/development-coconut-industry-growth-areas-province-quezon). <https://www.searca.org/projects/research/development-coconut-industry-growth-areas-province-quezon> (12 December 2023).

Sykas, D., 2020: The effects of the soil surface roughness and soil moisture content on the soil spectral signatures. [Geo.University](https://www.geo.university/pages/blog?p=how-spectral-signatures-are-affected-by-soil-variations). <https://www.geo.university/pages/blog?p=how-spectral-signatures-are-affected-by-soil-variations> (24 May 2024).

Tañada, E. L. M., Belen, E., Guerero, J., Pagkalinawan, H. M., & Blanco, A. C. (2023). *Mapping of Coconut in the Philippines Using Landsat 8 Images* [Unpublished manuscript]. Department of Geodetic Engineering, University of the Philippines – Diliman.

Vermote, E. F., Skakun, S., Becker-Reshef, I., & Saito, K., 2020: Remote sensing of coconut trees in Tonga using very high spatial resolution WorldView-3 data. *Remote Sensing* 12(19), 3113. doi.org/10.3390/RS12193113.

Xi, Y., Zhang, W., Brandt, M., Tian, Q., & Fensholt, R. (2023). Mapping tree species diversity of temperate forests using multi-temporal Sentinel-1 and -2 imagery. *Science of Remote Sensing*, 8(100094), 100094. doi.org/10.1016/j.srs.2023.100094.

Zheng, J., Yuan, S., Wu, W., Li, W., Yu, L., Fu, H., & Coomes, D., 2023: Surveying coconut trees using high-resolution satellite imagery in remote atolls of the Pacific Ocean. *Remote Sensing of Environment*, 287, 113485. doi.org/10.1016/j.rse.2023.113485.